

EFFECT OF POROSITY ON THE THERMO-MECHANICAL BENDING ANALYSIS OF FUNCTIONALLY GRADED RECTANGULAR PLATES (FGRP)

Hakima BELGHOUL¹, Slimane MERDADI^{2*}, Adda HADJ MOSTEFA³ and Ali BOUCHAFA⁴

¹University of Belhadj Bouchaib of Ain Témouchent, Faculty of Technology, Department of mechanical engineering, Laboratory engineering and sustainable development, Alegria. E-mail: Hakima.belghoul@univ-temouchent.edu.dz, hakouming@gmail.com

²University of Djillali Liabès of Sidi Bel Abbès, Faculty of Technology, Department of Civil Engineering and Public Works, Algeria. E-mail: slimanem2016@gmail.com

³Institute of Science & Technology, Civil Engineering Department, University of Relizane, Cité Bourmadia 48000 Relizane, Algeria. E-mail: addahadjmostefa@yahoo.fr

⁴University of Djillali Liabès of Sidi Bel Abbès, Faculty of Technology, Department of Civil Engineering and Public Works, Algeria. E-mail: bouchafa2006@yahoo.fr

AJME 2025, 23 (2); <https://doi.org/10.5281/zenodo.15863997>

ABSTRACT: This study examines the impact of porosity on the thermo-mechanical bending analysis of functionally graded rectangular plates (FGRP). The current theory suggests that only four unknown functions are involved, compared to five in other shear deformation theories, and the boundary conditions on the upper and lower surfaces of the plate do not require shear correction factors. It is assumed that the material properties of this plate (FGRP) vary continuously over the thickness of the plate according to a power law function in terms of the volume fractions of the constituents. The porosity distribution of the plates (FGRP) is uniform over their cross-sections. Using the concept of virtual work, the equilibrium equations of a plate (FGRP) are derived. Numerical results for the rectangular plates have been provided and compared to those found in the literature. The impact of aspect ratios and porosity volume on the bending and thermo-mechanical properties of the rectangular plates (FGRP) is examined.

KEYWORDS: Analytical solutions, Functionally graded, (FGRP), Thermo-mechanical, Bending, Porosity.

1 INTRODUCTION

Functionally graded materials (FGMs) are an advanced type of composite material whose composition and microstructure vary progressively with location. This design ensures the structure has optimal mechanical and thermal performance. Recently, FGMs, which have compositions and structures that gradually change over the volume, resulting in corresponding changes in mechanical and thermal properties, have been widely used. Due to the significance and applications of FGM structures, understanding their responses is crucial. Several studies have analyzed the thermo-mechanical behavior of FG plates.

According to the literature, many researchers have discussed shear deformation theories such as first-order higher shear deformation theories developed by (Whitney et al., 1970) and (Nguyen et al., 2008), third-order shear deformation theory

studied by (Reddy, 2000), and sinusoidal shear deformation theory presented by (Zenkour, 2006).

This study models the thermo-mechanical behavior of both perfect and imperfect functionally graded rectangular plates (FGRP) under bending, employing a higher-order theory for normal and shear deformation. The material properties of these porous rectangular plates are influenced by varying temperature loads. The analysis of perfect and imperfect FGRP is conducted using the principle of virtual work according to the current theory, taking into account both porosity and thermal effects. Various parameters, including the porosity factor, are examined. The results obtained are then compared with findings from other researchers.

2 METHODS AND THEORETICAL MODEL

In this investigation, the power law function is used. The following is the application of power law

distribution and the basic law of component mixture:

$$V(z) = \left(\frac{1}{2} + \frac{z}{h} \right)^k \quad (1)$$

Where 'k' is the power law index, a positive real integer, and 'z' is the distance from the mid-surface. Note that the volume fraction of ceramic is higher towards the upper surface of the plate and the volume fraction of metal is higher towards the bottom. Furthermore, according to equation (1), the upper surface of the plate ($z = h/2$) is ceramic, while the lower surface ($z = -h/2$) is metal.

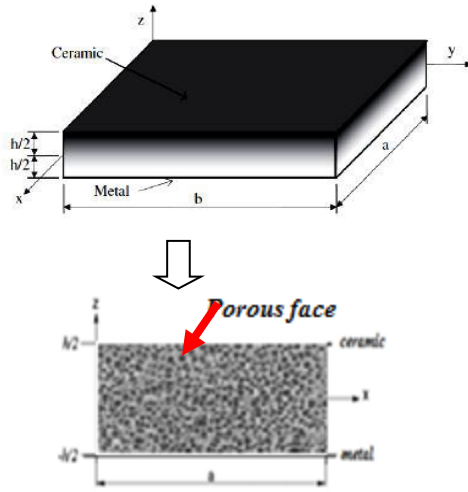


Fig. 1 Geometry of the porous rectangular plate (FGRP).

Based on the above assumptions, the displacement field is written as follows:

$$\begin{aligned} uu(xx, yy, zz) &= uu_0 - zz\phi_1 - f(z)\phi_2 \\ vv(xx, yy, zz) &= vv_0 - zz\phi_3 - f(z)\phi_4 \quad (2) \\ ww(xx, yy, zz) &= w_{bb} + w_{ss} \end{aligned}$$

$$\phi_1 = \frac{\partial w_b}{\partial x}, \quad \phi_2 = \frac{\partial w_s}{\partial x}, \quad \phi_3 = \frac{\partial w_b}{\partial y}, \quad \phi_4 = \frac{\partial w_s}{\partial y} \quad (3)$$

In this study the new function $f(z)$ is presented in the following form:

$$f(z) = z - \frac{z}{2} \left(\frac{h^2}{4} - \frac{z^2}{3} \right), \quad g(z) = 1 - f'(z) \quad (4)$$

In this study, an imperfect functionally graded (FG) material with a volume fraction of porosity, $P(\chi)$, ($0 \leq P(\chi) \leq 1$) is considered, distributed uniformly between metal and ceramic.

$$E(z) = E_m - \frac{P(\chi)}{2} (E_c + E_m) + (E_c - E_m) V(z) \quad (5)$$

E_c and E_m represent the properties of ceramics and metal, respectively. This power-law assumption

reflects a basic rule of mixtures used to determine the effective properties of the ceramic-metal plate.

The static equations can be derived using the principle of virtual displacements, which can be expressed in its analytical form as:

$$\int (\delta U + \delta V) = 0 \quad (6)$$

Where δU is the variation of the strain energy; δV is the variation of the potential energy. The virtual displacements concept may be used to get the static equations. In its analytical form, it may be expressed as

$$\delta U = \int_{-h/2}^{h/2} \int_A \left[\sigma_x \delta \varepsilon_x + \sigma_y \delta \varepsilon_y + \tau_{xy,1} \delta \gamma_{xy,1} + \tau_{yz,2} \delta \gamma_{yz,2} + \tau_{zx,3} \delta \gamma_{zx,3} \right] dA dz \quad (7)$$

$$\delta V = - \int_A q (\delta w_b + \delta w_s) dA \quad (8)$$

Where A is the upper surface.

It can be observed that the displacement field in Eq. (2) involves only four unknowns (u_0 , v_0 , w_s and w_b). Linear deformations can be expressed as:

$$\begin{Bmatrix} \varepsilon_x \\ \varepsilon_y \\ \gamma_{xy} \end{Bmatrix} = \begin{Bmatrix} \frac{\partial u_0}{\partial x} \\ \frac{\partial v_0}{\partial y} \\ \frac{\partial u_0}{\partial y} + \frac{\partial v_0}{\partial x} \end{Bmatrix} - z \begin{Bmatrix} \frac{\partial^2 w_b}{\partial x^2} \\ \frac{\partial^2 w_b}{\partial y^2} \\ 2 \frac{\partial^2 w_b}{\partial x \partial y} \end{Bmatrix} + f(z) \begin{Bmatrix} \frac{\partial^2 w_s}{\partial x^2} \\ \frac{\partial^2 w_s}{\partial y^2} \\ 2 \frac{\partial^2 w_s}{\partial x \partial y} \end{Bmatrix}, \quad (9a)$$

$$\begin{Bmatrix} \gamma_{yz} \\ \gamma_{xz} \end{Bmatrix} = \frac{df(z)}{dz} \begin{Bmatrix} \frac{\partial w_s}{\partial y} \\ \frac{\partial w_s}{\partial x} \end{Bmatrix}, \quad \varepsilon_z = 0 \quad (9b)$$

Eq. (10) may be used to write the component relations of a FG plate.

$$\begin{Bmatrix} \sigma_{xx} \\ \sigma_{yy} \end{Bmatrix} = \frac{E(z)}{1-\nu^2} \begin{bmatrix} 1 & \nu \\ \nu & 1 \end{bmatrix} \begin{Bmatrix} \varepsilon_{xx} - \alpha \Delta T \\ \varepsilon_{yy} - \alpha \Delta T \end{Bmatrix}, \quad (10a)$$

$$\begin{Bmatrix} \tau_{xy,1} \\ \tau_{yz,2} \\ \tau_{zx,3} \end{Bmatrix} = \frac{E(z)}{2(1+\nu)} \begin{Bmatrix} \gamma_{xy,1} \\ \gamma_{yz,2} \\ \gamma_{zx,3} \end{Bmatrix} \quad (10b)$$

where $(\sigma_{xx}, \sigma_{yy}, \tau_{xy,1}, \tau_{yz,2}, \tau_{zx,3})$ and $(\varepsilon_{xx}, \varepsilon_{yy}, \gamma_{xy,1}, \gamma_{yz,2}, \gamma_{zx,3})$ are the stress and strain components, respectively.

To address this issue, "Navier" assumes that the mechanical and thermal transverse loads $\{q\}$ and

$\{T\}$, are represented as a double fourier series in the form of:

$$\begin{Bmatrix} q \\ T \end{Bmatrix} = \begin{Bmatrix} q_{00} \\ t_{ii} \end{Bmatrix} \sin(\lambda\lambda x) \sin(\mu\mu y) \quad (11)$$

The following type of solution is assumed for applying the Navier solution procedure.

$$\begin{Bmatrix} UU \\ VV \\ W_b \\ W_s \end{Bmatrix} = \begin{Bmatrix} UU_{mn} \cos(\lambda\lambda x) \sin(\mu\mu y) \\ VV_{mn} \sin(\lambda\lambda x) \cos(\mu\mu y) \\ W_{bmn} \sin(\lambda\lambda x) \sin(\mu\mu y) \\ W_{smn} \sin(\lambda\lambda x) \sin(\mu\mu y) \end{Bmatrix} \quad (12)$$

Where: UU , VV , W_b & W_s are arbitrary parameters to be determined with:

$\lambda\lambda = m\pi/a$ and $\mu\mu = n\pi/b$, « m » and « n » are mode numbers.

3 NUMERICAL RESULTS AND DISCUSSION

Zirconia & titanium, as shown in Table 1, were the materials taken into consideration.

Table 1. Provides the material parameters that were utilized to make the FG plate.

Properties	(Titanium, Ti-6Al-4V)	(Zirconia, ZrO ₂)
E (Pa)	66.2*10 ⁹	117.0*10 ⁹
ν	0.33	0.33
α	10.3 ×(10 ⁻⁶ / °C).	7.11 ×(10 ⁻⁶ / °C).

The current deflection results for the perfect FG square and rectangular plate are very similar to the results of other theories (Zenkour et al., 2019 & Belkorissat et al., 2023) present in the Table 2. It is shown that the deflections values and rise with increasing heat loads (t_{22}).

Table 2: The deflection of Perfect P-FGM square and rectangular plates ($k=2$, $t_{33}=0$)

Theory	$t_{22} = 0$		$t_{22} = 100$	
	$a=b$	$3a=b$	$a=b$	$3a=b$
Zenkour et al. 2019	0.3729	1.1820	7.2408	13.4032
Belkorissat et al. 2023	0.3781	1.1958	6.9668	13.0560
Present	0,37959	1.19845	6.96730	13.0577

From Table 3, again, the deflection and stresses results of FGRP subjected to a mechanical load compare very well with the theory solutions (FSDT

by (Whitney et al. 1970), TSDT (Reddy et al. 2000) and SSDT (Zenkour et al. 2006)) for (FGRP) are consistent, it demonstrates the present model's validity. It is evident that the deflection and stress levels escalate with the increase in porosity values $P(\chi)$.

Table 3. Comparisons of deflections and stresses of perfect and imperfect (FGRP), with ($T = 0$, $k=0$).

Theory	\bar{w}	$\bar{\sigma}_x$	$\bar{\tau}_{xz,3}$	$\bar{\tau}_{xy,1}$
Whitney et al. 1970	0,85892	0,51065	0,72949	-0,34377
Reddy et al. 2000	0,85891	0,51545	0,72797	-0,42956
Zenkour et al. 2006	0,85887	0,51362	0,72784	-0,44327
Present ($P(\chi)=0.0$)	0,85889	0,51346	0,72796	-0,42955
Present ($P(\chi)=0.1$)	0,93185	0,513457	0,727954	-
Present ($P(\chi)=0.2$)	1,01835	0,513459	0,727961	-0,42955
Present ($P(\chi)=0.3$)	1,12255	0,513458	0,727961	-

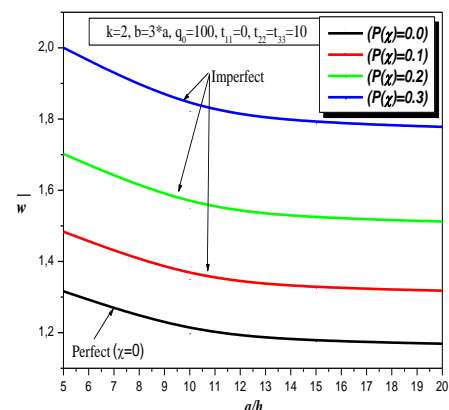
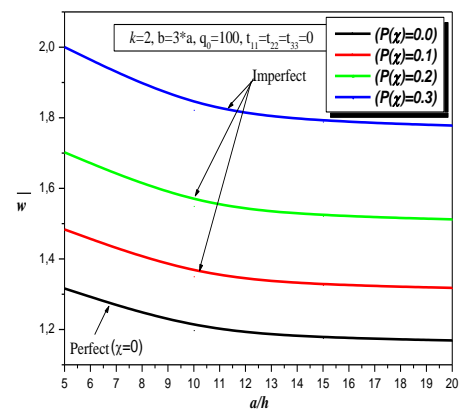


Fig. 2. Variation of deflection versus (a/h) for rectangular plate (FGRP).

Fig. 2. illustrates how the deflection changes for various side-to-thickness ratios and porosity coefficient of perfect and imperfect and with/without a thermal load for (FGRP). For the (FGRP), the deflection of the (FGRP) decreases as the (a/h) increases. When the porosity parameter is increased under a thermal load, deflection decreases for some side-to-thickness ratio values.

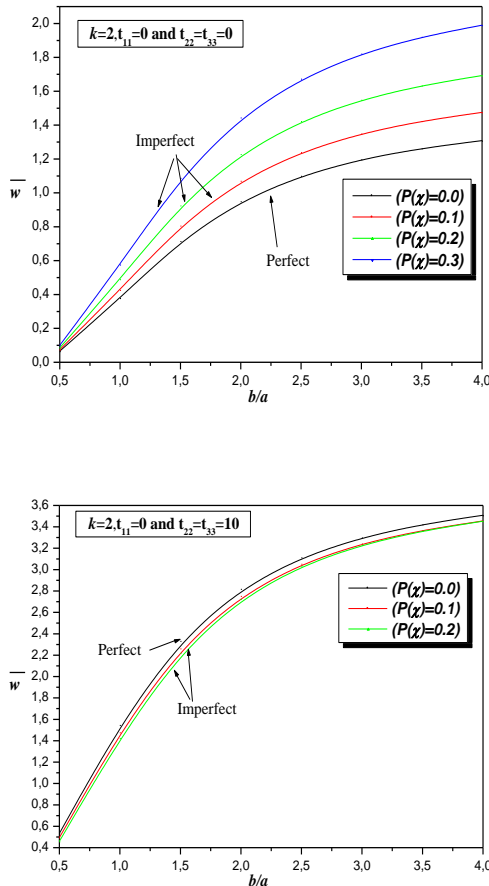


Fig. 3. Variation of deflection versus aspect ratio for rectangular plate (FGRP).

For (FGRP), as well as with and without thermal loads, we investigate deflection variation as a function of the geometric ratio (b/a) , for a $(a/h = 10)$ and a power law index $(k = 2)$, as shown in Fig.3. The results show that for both perfect and defective rectangular plate (FGRP), the deflection increase as the aspect ratio rises. We can see in this figure which effects thermal load has on the different aspect ratios (b/a) and which effects porosity has on those ratios. The thermal load has the most significant effects, while the porosity effects as significant.

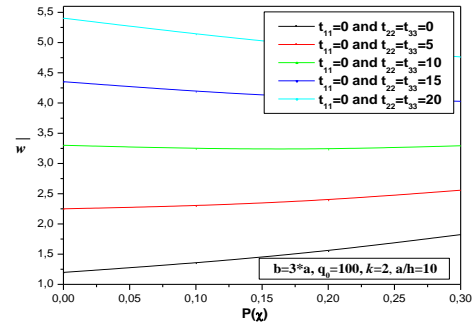


Fig. 4. Variation of deflection versus of the porosity coefficient and different thermo-mechanic loading for rectangular plate (FGRP).

Figure 4. illustrates how decreasing the dimensionless deflections of both perfect and imperfect rectangular plate (FGRP) is possible by raising the porosity parameter and thermo-mechanic loading. Furthermore, for the same value of the porosity parameter, the dimensionless deflection in the case of thermal load $(t_{22}=t_{33}=20)$ is larger than that in the cases of $t_{22}=t_{33}=5, 10$ and 15 . This is mostly because of where the porosity is and how important thermal loading is.

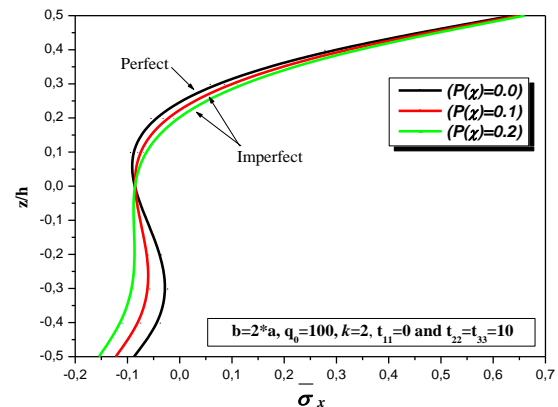


Fig. 5. Variation of axial stress and shear stress across the thickness of (FGRP).

Numerical results for FGM rectangular plates with different aspect ratios and porosity levels are presented. The results show that both the aspect ratio and the porosity significantly influence the bending and thermomechanical behavior of the plates. Plates with higher porosity levels exhibit lower stiffness and higher deflections under the same loading conditions. The temperature also plays a crucial role, with higher temperatures leading to increased deflections and stresses in the plates.

4 CONCLUDING REMARKS

The study concludes that the higher-order shear deformation theory is effective for analyzing the thermo-mechanical behavior of FGM plates with varying porosity. The results highlight the importance of considering both porosity and temperature effects in the design and analysis of FGM structures. Future research could focus on more complex loading conditions and the use of different FGM compositions to further understand their behavior.

5 REFERENCES

- Belkorissat, I., Ameer, M. (2023). *Influence of an initial imperfection on hygro-thermo-mechanical behaviors of FG plates laid on elastic foundation*, Journal of Mechanical Science and Technology 37(5) 2471- 2477.
- Hadj Mostefa, A., Bouchafa, A., Merdaci, S. (2021). *Dynamic Behavior Study of Functionally Graded Porous Nanoplates*. Nano Hybrids and Composites, 33, 83-92.
- Merdaci, S., Belghoul, H. (2019). *High Order Shear Theory for Static Analysis Functionally Graded Plates with Porosities*. Comptes rendus Mécanique, 347(3), 207-217.
- Merdaci, S., Hadj Mostefa, A., Beldjelili, Y., Merazi, M., Boutaleb, S., Hellal, H. (2021). *Analytical solution for static bending analysis of functionally graded plates with porosities*, Frattura ed Integrità Strutturale, 55, 65-75.
- Nguyen, T.K., Sab, K., Bonnet, G. (2008). *First order shear deformation plate models for functionally graded materials*, Compos.Struct, 83, 25–36.
- Reddy, J.N. (2000). *Analysis of functionally graded plates*, Int.J.Numer.Methods Eng,47, 663–684.
- Whitney, J.M., Pagano, N.J. (1970). *Shear deformation in heterogeneous anisotropic plates*, ASMEJ.Appl.Mech, 37, 1031–1036.
- Zenkour, A.M. (2006). *Generalized shear deformation theory for bending analysis of functionally graded plates*, Appl.Math.Model, 30, 67–84.
- Zenkour, A. and Radwan, A. (2019). *Bending response of FG plates resting on elastic foundations in hygrothermal environment with porosities*, Composite Structures, 213, 133-143.

6 NOTATION

The following symbols are used in this paper:

a: length of the plate

b: width of the plate

E_c : material properties of the ceramic

E_m : material properties of the metal

$f(z)$: warping function (transverse shear function)

$f'(z)$: first derivative of the warp function with respect to z

h: total thickness of the plate

k : power-law index

$V(z)$: volume fraction

w: transverse displacement

w_{bb} : bending components

w_{ss} : shear components

xx, yy, zz: coordinates

ν : Poisson's ratio

$P(\chi)$: porosity volume fraction

uu, vv, ww : displacement in the x,y and z directions, respectively

u_0, v_0, w_0 : mid-plane displacements in x,y and z directions

$\gamma_{xy}, \gamma_{yz}, \gamma_{zx}$: distortion deformation

$\epsilon_{xx}, \epsilon_{yy}$: deformation in the x, y direction

σ_{xx}, σ_{yy} : normal stresses

$\tau_{xy}, \tau_{yz}, \tau_{zx}$: shear stress